Journal of Zhejiang University-SCIENCE A (Applied Physics & Engineering)
ISSN 1673-565X (Print); ISSN 1862-1775 (Online)
www.zju.edu.cn/jzus; www.springerlink.com
E-mail: jzus@zju.edu.cn

Aerodynamic modeling and stability analysis of a high-speed train under strong rain and crosswind conditions*

Xue-ming SHAO[1], Jun WAN[1], Da-wei CHEN[2], Hong-bing XIONG[†‡1]

([1]*Department of Mechanics, Zhejiang University, Hangzhou 310027, China*)

([2]*National Engineering Laboratory for System Integration of High-Speed Train (South), CSR Qingdao Sifang Co., Ltd., Qingdao 266111, China*)

[†]E-mail: hbxiong@zju.edu.cn

Received Sept 23, 2011; Revision accepted Sept 24, 2011; Crosschecked Sept 24, 2011

Abstract: With the development of high-speed train, it is considerably concerned about the aerodynamic characteristics and operation safety issues of the high-speed train under extreme weather conditions. The aerodynamic performance of a high-speed train under heavy rain and strong crosswind conditions are modeled using the Eulerian two-phase model in this paper. The impact of heavy rainfall on train aerodynamics is investigated, coupling heavy rain and a strong crosswind. Results show that the lift force, side force, and rolling moment of the train increase significantly with wind speed up to 40 m/s under a rainfall rate of 60 mm/h. when considering the rain and wind conditions. The increases of the lift force, side force, and rolling moment may deteriorate the train operating safety and cause the train to overturn. A quasi-static stability analysis based on the moment balance is used to determine the limit safety speed of a train under different rain and wind levels. The results can provide a frame of reference for the train safe operation under strong rain and crosswind conditions.

Key words: High-speed train, Aerodynamic characteristics, Multiphase flow, Rain, Crosswind, Overturning
doi:10.1631/jzus.A11GT001 **Document code:** A **CLC number:** O359; TD524

1 Introduction

When high-speed trains running under strong rain and crosswind conditions, especially at exposed locations such as bridges or embankments, the aerodynamic forces and moments may increase significantly and result in the train instability. It was well-known that the strong crosswind may increase the aerodynamic drag force, side force and yawing moment. If the rain and the crosswind coexist, the aerodynamic performance of train will deteriorate more severely, which may cause train delays, shutdowns, derailments and even overturning. In 2007, trains derailed with 11 cars under high wind conditions, causing a serious accident on the Xinjiang Railway South Line and a train overturned in Tianjin (Fig. 1a). In Japan, there have been about 30 wind-induced accidents to date (Fig. 1b).

Numerous studies have been done on the aerodynamic performance of trains under crosswind conditions. Ma *et al*. (2009) investigated the aerodynamic characteristics of a train on a straight line at 350 km/h with a crosswind. More systematic researches on numerical simulation of a train travelling along a straight line and also curves have been done (Liang and Shen, 2007; Yang *et al*., 2010). In addition to wind tunnel experiments, numerical simulation analyzes the effects of crosswinds in more detail with results consistent with those from experiments (Christina *et al*., 2004; Javier *et al*., 2009; Sanquer *et al*., 2004; Masson *et al*., 2009). However, less attention has been paid to the effects of combined strong rain and crosswind on the aerodynamic characteristics

‡ Corresponding author
* Project (No. 2009BAG12A01-C03) supported by the National Key Technology R&D Program of China

and safety of high-speed trains. This paper deals with the influence of strong rain and crosswind conditions on high-speed train aerodynamics, based on numerical simulations. A quasi-static stability analysis based on the moment balance is also used to determine the limit safety speed of a train under different rain and wind levels, which provides some guidance for the train operation safety.

Fig. 1 Train overturning in China (a) and Japan (b)

2 Numerical simulation

2.1 Computational model

Computational fluid dynamics (CFD) software FLUENT is used for numerical simulation in this study. For multiphase flow problems, there are mainly two types of multiphase flow models: one is the discrete particle model (DPM) proposed by Crowe and Smoot (1979); the other one is Eulerian-Eulerian model proposed by Gidaspow (1994). The fluid phase in DPM is solved using the Eulerian method, while the granular phase is tracked by the Lagrangian method. Though providing more detail, DPM is not suitable for large-scale engineering simulation with numerous dispersed particles, due to the limitation of finite memory capacity and CPU efficiency. The Eulerian-Eulerian approach is more efficient and usually more complex. Each phase is treated as a continuous medium that may interpenetrate with other phases, and is described by a set of equations with regard to momentum, continuity, and energy. The Eulerian-Eulerian approach has been successfully applied to the simulation of gas-particle multiphase flow with a large number of particles in large equipment. For example, Liu *et al.* (2006) studied the liquid-solid slurry transport within a pipeline, and Cao *et al.* (2005) simulated the bubble growth, integration, and the flow characteristics in a fluidized bed. Due to these advantages, the Eulerian-Eulerian model is used to simulate the example in this study.

The flow around the train is viscous, turbulent, and gas-droplet two-phase flow. Thus, the Eulerian-Eulerian multiphase model coupling with the k-ε turbulence equation is used for the gas-droplet two-phase flow field around the train. Details of the Eulerian-Eulerian multiphase model and its validation could be found in another paper of this issue (Xiong *et al.*, 2011) conducted in our group.

2.2 Computational domain

A simplified model of CRH2 (China Railway High Speed 2) is studied, including three coaches of the head, middle and tail. To fully develop flow around the train and to ensure the accuracy of results, a large semi-cylindrical numerical wind tunnel was established as the computational domain (Fig. 2). The distances of the semi-cylindrical computational domain in the vertical, horizontal and vertical directions are 600, 400 and 200 m, respectively. The length of vehicle is 76 m. The distance between nose of vehicle and the inlet boundary is 100 m. Direction of the flow field is at the positive x-axis.

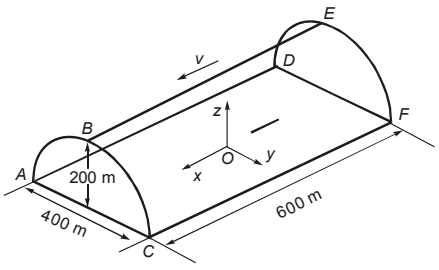

Fig. 2 Computational domain

2.3 Computational mesh

The computational domain is meshed with the hexahedral structured grid, with refine mesh on the

front and rear of the train and surrounding areas as shown in Fig. 3. To validate the train model via numerical simulation, grid dependency has been conducted with three kinds of grid generation: 330000, 600000, 980000 grids, as shown in Table 1, where the change rate Δ is defined as

$$\Delta = \frac{F_i - F}{F}, \tag{1}$$

where F_i is the aerodynamic force (or moment) for different mesh models, and F is the aerodynamic force with 98000 grids. The results of 980000 grids are very close to that of 60000 grids. Therefore, we can conclude that 980000 grids are acceptable for the numerical simulation of the train.

2.4 Boundary conditions

Planes DEF and ABCFED in the computational domain (Fig. 2) are given as the boundaries of velocity inlet. Plane ABC is a pressure outlet boundary with a static pressure of 0. Train surfaces are stationary, with non-slip boundary condition.

Plane ACFD adopts a moving boundary with speed equal to flow velocity. The crosswind direction is on the positive y-axis, perpendicular to the train. The continuous phase and the granular phase sets are as follows: the continuous phase uses inlet boundary velocity of 360 km/h; the granular phase uses inlet boundary with x-axis velocity equal to the gas inlet velocity and negative z-axis velocity of raindrop of 5 m/s. Turbulent kinetic energy k and turbulent dissipation rate ε are determined by

$$k = 0.004 u_{\mathrm{m}}^2 \tag{2}$$

$$\varepsilon = 0.09 \frac{k^{1.5}}{0.03R}, \tag{3}$$

where u_{m} is the mean flow velocity, and R is the turbulence length scale. The Phase-Coupled-Simple algorithm is used for solving the coupling between pressure and velocity effects (Moukalled *et al*., 2003).

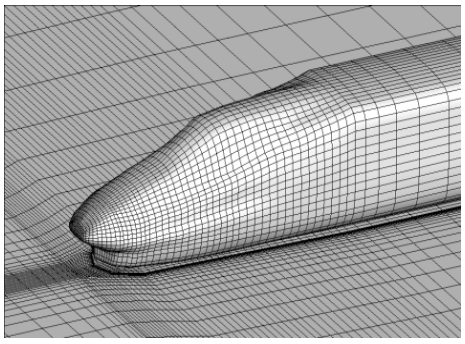

Fig. 3 Computational mesh

3 Problem description

In this study, the train running speed is set as 360 km/h. The crosswind speed ranges from 0 to 40 m/s, and the direction of wind is perpendicular to the running direction of train. Under the crosswind and heavy rainfall computing conditions, rainfall rate (rainfall intensity per hour) is 60 mm/h. A raindrop is regarded as spherical with constant falling velocity of 5 m/s and diameter of 0.002 m.

4 Results and discussion

4.1 Pressure distribution on the train surface

The drag force on the train consists of pressure drag and friction drag. The pressure drag increases dramatically when running at high speed. Due to the impact of rainfall, the pressure distribution around the

Table 1 Aerodynamic comparison in different grid models

Mesh model	Drag force (N)	Δ	Side force (N)	Δ	Lift force (N)	Δ
330000	19945.18	7.6%	56.96	60.3%	7686.27	−1.2%
600000	19018.51	2.6%	36.27	2.1%	7747.46	−0.4%
980000	18528.52	0	35.53	0	7782.27	0%
Mesh model	Rolling moment (N·m)	Δ	Pitching moment (N·m)	Δ	Yawing moment (N·m)	Δ
330000	4552.40	−1.8%	−565823	5.9%	13900.92	12.9%
600000	4616.65	−0.5%	−541518	1.4%	12571.86	2.1%
980000	4637.63	0	−534160	0	12317.19	0

train may be more complex when the train runs in the rain conditions. By analyzing the pressure distribution around the train, it is helpful to understand the mechanism of the aerodynamic characteristics on the train.

The pressure distribution of the train under crosswind of 30 m/s and rainfall rate of 60 mm/h is shown in Fig. 5. For the head vehicle (Fig. 5a), the maximum pressure occurs at the front of the nose and the windward side of the head vehicle. The negative pressure appears at the leeward side of the vehicle window, which will cause a side force along the wind direction. If the side force is large enough, it may lead to train derailment. Pressure on the tail vehicle is opposite to the head vehicle as shown in Fig. 5b. The largest negative pressure occurs on the windward side of the rear window transition zone, and the positive pressure occurs on the leeward side of the window transition zone and tail vehicle nose. This makes side force of tail vehicle reverse the direction of head train. As the side forces of head vehicle and tail vehicle are in the opposite direction, the train will have a yawing moment, and this may bring a risk of train derailment.

4.2 Aerodynamic force of train under strong rain and crosswind conditions

Side force under no rain and rain conditions are shown in Fig. 6a for different crosswind speeds. It could be seen that the side force increases with wind speed. Due to the effect of rain, the side force under the rain condition is larger than that under no rain condition. Side force is mainly caused by the pressure difference on the two sides of the train. The effect of rain on side force is significant, and increases the risk of derailment.

The lift force under no rain and rain conditions are shown in Fig. 6b. It can be seen that the lift force increases with wind speed. For the rain condition, the lift force is larger than that under no rain condition, increasing the risk of derailment.

Drag force under no rain and rain conditions are shown in Fig. 6c. Drag force increases first, reaching a maximum value when the wind speed reaches about 15 m/s, and then decreases with wind speed. This is due to the drag force of the first vehicle decreasing with wind speed, and even changing force direction as negative drag, though the drag force of the tail vehicle always increases with wind speed.

These three force components have different effects on the train stability and safety. Generally, the side force increases the wheel-track load on the leeward side and the wheel-rail contact force. Large side forces worsen the wear of the wheel and rail, and may cause train derailment, or even overturning. The negative lift force increases axle load and also exacerbates the wear of track and wheel; the positive lift force floats the train, and large positive lift force may cause train derailment. Drag force increases rapidly with an increase of train speed, requiring more energy consumption and increasing the air noise.

4.3 Aerodynamic moment of train under strong rain and crosswind conditions

Fig. 7a illustrates the train rolling moments under no rain and rain conditions. Rolling moment increases with wind speed and has a larger absolute value if considering the influences of rain. This means that the train derailments are more likely to happen under heavy rainfall conditions. Pitching moments

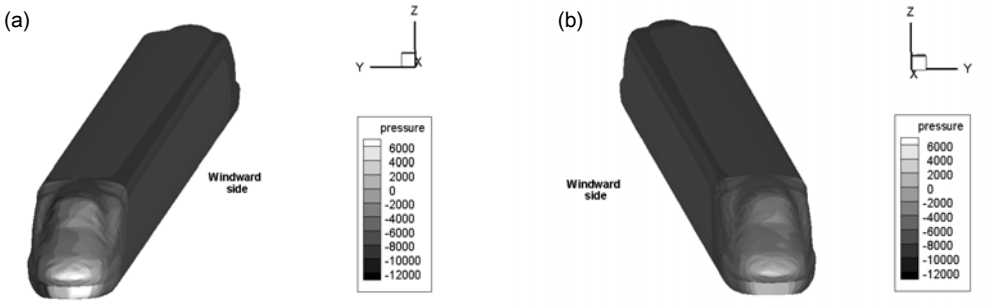

Fig. 5 Pressure on the train. (a) Front view; (b) Rear view (Unit: Pa)

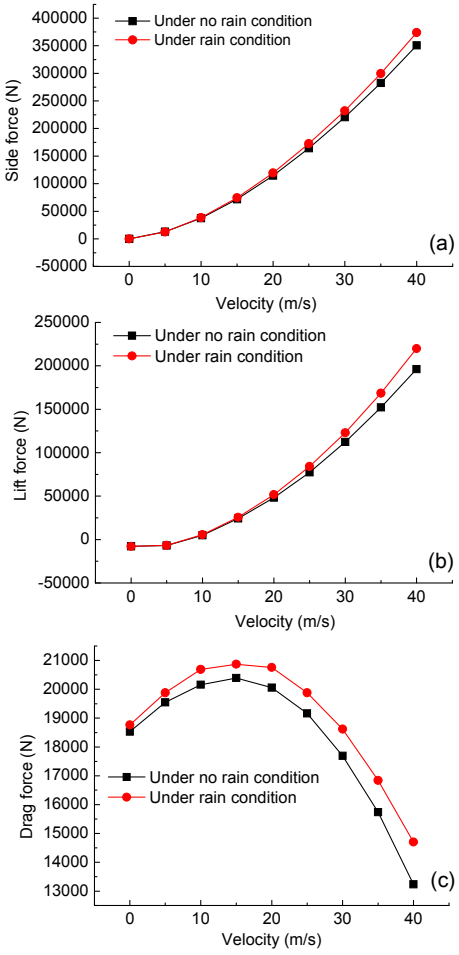

Fig. 6 Side (a), lift (b) and drag force (c) of the train

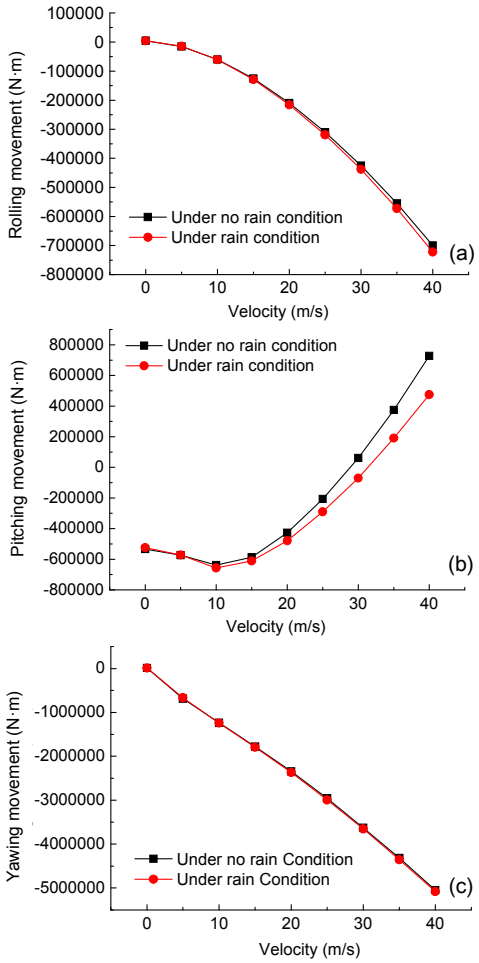

Fig. 7 Rolling (a), pitching (b) and yawing moment (c) of the train

under the heavy rainfall and no rainfall conditions are plotted in Fig. 7b. Results show that the pitching moments, in the direction of nose-down, increase slightly with wind speed under 10 m/s, and then decrease when the wind speed continually increases. The pitching moments reverse their direction as nose-up at the wind speed of about 30 m/s, and then monotonically increase with wind speed. Fig. 7c illustrates the train yawing moments under no rain and rain conditions. The yawing moment has no detectable change in the conditions of rain and no rain. In both case, the yawing moments increase with the wind speed, mainly resulting from the large side force in the windward direction.

In the three components of train moment, the rolling moment is mostly important for the train safety, which increases the risk of overturning. The less important one is the yawing moment, which makes the train swing around the axle and increases the tendency to derail. If the train is subject to intermittent wind gusts, the large yawing moment may cause train vibration and worsen passenger comfort. The minor parameter for train safety is the pitching moment, which makes the train move up and down and affects passenger comfort mainly.

4.4 Stability analysis of the train under rain and crosswind conditions

Stability analysis of the train overturning is used to evaluate the train speed limit when running on the straight or curved rails considering the effects of strong rain and crosswind. When running on curved rails, the outer rail has an excessive height compared to the inner rail and an unbalanced centrifugal force will be generated. There are three kinds of turnover: (1) Running on a straight rail, the train turn over in the

windward direction; (2) Running on a curved rail, the train turn over toward the outside rail with wind blowing from the inside rail; (3) Running on a curved rail, the train turn over toward the inside rail with wind blowing from the outside rail.

The running stability of the train concludes the shape of the train, size of the train, mass of the train, the height of center of gravity, running speed and so on. The relationship of limit running speed and crosswind speed can be derived from the dynamic torque balance principle. The method and formulae have been studied (Gao and Tian, 2004; Tian, 2007). This method is used in this study to calculate the limit running speed of train under rain conditions.

According to the cases listed in Table 2, we calculated the lift force coefficient c_l, side force coefficient c_s, and rolling moment coefficient c_m at different yaw angles. These data are then processed to fit the relationship between yaw angle (α) and c_l, c_s, and c_m as follows:

Table 2 Computing conditions at different yaw angles

Working condition	Yaw angle (°)*	Rainfall rate (mm/h)
1	0	70
2	30	70
3	45	70
4	60	70
5	75	70

* Yaw angle is defined as the angle between the train velocity vector and the resultant velocity vector

Under no rain condition:

$$c_l=-1.2901\times10^{-6}\alpha^3+1.5166\times10^{-4}\alpha^2+2.9972\times10^{-3}\alpha,$$
$$c_s=-1.2310\times10^{-6}\alpha^3+1.1188\times10^{-4}\alpha^2+8.2266\times10^{-3}\alpha,$$
$$c_m=-2.6019\times10^{-7}\alpha^3-5.7588\times10^{-6}\alpha^2+7.2329\times10^{-3}\alpha.$$

Under rain condition:

$$c_l=-1.2183\times10^{-6}\alpha^3+1.3945\times10^{-4}\alpha^2+3.8124\times10^{-3}\alpha,$$
$$c_s=-9.4652\times10^{-7}\alpha^3+7.4161\times10^{-5}\alpha^2+9.8655\times10^{-3}\alpha,$$
$$c_m=-9.4652\times10^{-7}\alpha^3+7.4161\times10^{-5}\alpha^2+9.8655\times10^{-3}\alpha.$$

Finally, taking these formulae into the moment balance analysis, the limit speeds of the train running in the straight and curve rails were calculated. Results are listed in Table 3 for no rain condition and Table 4 for rain condition.

We could see from Table 4 that under heavy rain and crosswind, the yaw angle increases as the wind speed increases, and the critical speed of the train decreases. When the train is running on a curve, the critical running speed of the train caused by wind blows from the outside is smaller than that caused by wind blows from the inside, which means it is more easily to overturn on the inner curve track. The critical running speed of a train running on a straight line is larger than that on a curve line when the wind blows from the outside rail to the inside rail, but smaller than that on a curve line when the wind blows from the

Table 3 Relationship between train running safety speed and side wind speed under no rain condition

α (°)	Overturning on line		Overturning on outer curve line		Overturning on inner curve	
	Wind speed (m/s)	Train speed (m/s)	Wind speed (m/s)	Train speed (m/s)	Wind speed (m/s)	Train speed (m/s)
15	20.600	76.922	26.346	98.376	17.355	64.805
30	27.883	48.325	30.987	53.703	25.451	44.110
45	32.454	32.480	34.728	34.756	30.484	30.508
60	35.326	20.420	37.193	21.500	33.635	19.443
75	36.934	9.923	38.599	10.370	35.393	9.509
90	37.601	0.030	39.227	0.031	36.092	0.029

Table 4 Relationship between train running safety speed and side wind speed under heavy rain

α (°)	Overturning on line		Overturning on outer curve line		Overturning on inner curve	
	Wind speed (m/s)	Train speed (m/s)	Wind speed (m/s)	Train speed (m/s)	Wind speed (m/s)	Train speed (m/s)
15	17.617	65.783	20.897	78.031	15.425	57.596
30	23.484	40.701	25.338	43.913	21.913	37.977
45	27.006	27.027	28.381	28.404	25.753	25.774
60	29.101	16.822	30.239	17.480	28.032	16.204
75	30.149	8.100	31.161	8.372	29.183	7.840
90	30.411	0.024	31.383	0.025	29.479	0.023

inside rail to the outside rail. Comparing to the condition of crosswind without rain, the train limit speeds decrease about 10%–20%, which means that the train is more easily to overturn under strong rain condition.

5 Conclusions

Research studies have been focused on the train aerodynamic behaviors under rain and crosswind conditions, using the Eulerian-Eulerian two-phase model. Compared to no rain condition, the drag force, side force, and lift force increase under rain conditions. For high crosswind velocities, the effects of rain on aerodynamic behavior are more apparent. The rolling moment in the rain is greater than that without the rain. The pitching moment changes obviously under rain condition. The yawing moment has no detectable change in the conditions of rain and no rain. The main factors affecting the train safety considerations are the side force, lift force, and rolling moment. A quasi-static stability analysis using the moment balance is used to determine the limit safety speed of train under different rain and wind levels. Results show that the train is more easily to overturn on the inner curve track. The train limit speeds under rain decrease about 10%–20% than that under no rain, which means that the train is more easily to overturn under strong rain condition.

References

Cao, Y., Li, X., Yan, J., 2005. Numerical simulation of dense gas-solid flow in pipe-type fluidized bed. *Journal of Zhejiang University (Engineering Science)*, **39**(6):1-6 (in Chinese).

Che, D.F., Li, H.X., 2007. Multiphase Flow and Its Application. Xi'an Jiaotong University Press, Xi'an, China, p.518-525 (in Chinese).

Christina, R., Thomas, R., Wu, D., 2004. Computational Modeling of Cross-Wind Stability of High Speed Trains. European Congress on Computational Methods in Applied Sciences and Engineering, Jyväskylä, p.1-20.

Crowe, C.T., Smoot, L.D., 1979. Multicomponent Conservation Equation. In: Pulverized-Coal Combustion and Gasification, Plenum Press, New York.

Gao, G.J., Tian, H.Q., 2004. Effect of strong cross-wind on the stability of trains running on the Lanzhou-Xinjiang railway line. *Journal of the China Railway Society*. **26**(4):36-41 (in Chinese).

Gidaspow, D., 1994. Multiphase Flow and Fluidization. Academic Press, Boston, America.

Javier, G., Jorge, M., Antonio, C., Aitor, B., 2009. Comparison of Experimental and Numerical Results for a Reference CAF Train Exposed to Cross Winds. Euromech Colloquium 509 Vehicle Aerodynamics, Berlin, Germany, p.82-92.

Liang, X.F., Shen, X.Y., 2007. Side aerodynamic performances of maglev train when two trains meet with wind blowing. *Journal of Central South University* **38**(4):1-6 (in Chinese).

Liu, Y.B., Chen, J.Z., Yang, Y.R., 2006. Numerical simulation of liquid-solid two-phase flow in slurry pipeline transportation. *Journal of Zhejiang University (Engineering Science)*, **40**(5):1-6 (in Chinese).

Ma, W.H., Luo, S.H., Song, R.R., 2009. Influence of cross-wind on dynamic performance of high-speed EMU on straight track. *Journal of Chongqing Institute of Technology*, **23**(3):1-5 (in Chinese).

Masson, E., Allain, E., Paradot, N., 2009. CFD Analysis of the Underfloor Aerodynamics of a Complete TGV High Speed Train Set at Full Scale. Berlin, Germany. Euromech Colloquium 509 Vehicle Aerodynamics, Berlin, Germany, p.188-202.

Moukalled, F., Darwish, M., Sekar, B., 2003. A pressure-based algorithm for multi-phase flow at all speeds. *Journal of Computational Physics*, **l90**(2):550-571. [doi:10.1016/S0021-9991(03)00297-3]

Sanquer, S., Barré, C., de Virel, M.D., Cléon, L.M., 2004. Effect of cross winds on high-speed trains: development of a new experimental methodology. *Journal of Wind Engineering and Industrial Aerodynamics*, **92**(7-8): 535-545. [doi:10.1016/j.jweia.2004.03.004]

Tian, H.Q., 2007. Train Aerodynamics. China Railway Publishing House, Beijing, China (in Chinese).

Xiong, H.B., Yu, W.G, Chen, D.W., Shao, X.M., 2011. Numerical study on the aerodynamic performance and safe running of high-speed trains in sandstorms. *Journal of Zhejiang University-SCIENCE A (Applied Physics and Engineering)*, **12**(12):971-978. [doi:10.1631/jzus.A11GT005]

Yang, Z.G., Ma, J., Chen, Y., 2010. The unsteady aerodynamic characteristics of a high-speed train in different operating conditions under cross wind. *Journal of the China Railway Society*, **32**(2):1-6 (in Chinese).